# A Case Study on Buckling Stability of Piles in Liquefiable Ground for a Coal-Fired Power Station in Indonesia

*by* Rini Kusumawardani

# A Case Study on Buckling Stability of Piles in Liquefiable Ground for a Coal-Fired Power Station in Indonesia

Muhammad Hamzah Fansuri[1(✉)], Muhsiung Chang[1], and Rini Kusumawardani[2]

[1] Department of Civil and Construction Engineering, National Yunlin University of Science and Tech (YunTech), Yunlin, Taiwan
ml06162l2@gemail.yuntech.edu.tw, changmh@yuntech.edu.tw

[2] Department of Civil Engineering, Universitas Negeri Semarang (Unnes), Semarang, Indonesia
rini.kusumawardani@mail.unnes.ac.id

**Abstract.** This paper discusses a case study on the assessment of buckling stability of piles due to liquefaction of foundation soils for a coal-fired power station (CFPS) in Indonesia. As the rapid growth in the economy sector, the demand for electricity is increasing and a CFPS is planned and constructed in Central Java. During the planning stage, the risk caused by earthquakes should be considered. As the foundation soils of the site consist of soft sandy silts or clays interbedded with loose fine sands up to a depth of 9 m, soil liquefaction and its effect on the buckling stability of piles for CFPS thus become the main concerns of this project. Liquefaction analysis is performed based on a SPT-N approach. A depth-weighted procedure is applied for the assessment of liquefaction potential for the site. Results of liquefaction assessment indicate the site is prone to risk of soil liquefaction due to the design earthquake. Buckling of piles due to seismic loading is evaluated for the cases of liquefied soils in both dry and wet seasons, while only the wet season scenario is the main focus of this paper. A buckling stability index $G$ is adopted as the difference between the critical pile length ($H_c$) for buckling and the unsupported pile length ($D_L$) due to soil liquefaction. If $G$ is greater than zero, then the pile is safe; otherwise, the pile will buckle. Results of buckling assessment show $G > 0$ for the piles of the site with an average $G$ value of 15 as the foundation soils are liquefied during the design earthquake with magnitude $M_w$ of 6.8, indicating the pile foundation of the CFPS should be safe from buckling failure due to soil liquefaction.

## 1 Introduction

Indonesia is one of the countries located in a highly seismic area. It is surrounded by the Trans-Asian and Circum Pacific belts. In addition, it is also surrounded by three major active tectonic plates, namely, Eurasia, Indo-Australian, and Philippine Plates. Due to the effect of the colliding plates, the region becomes actively tectonic and volcanic as well. The active tectonics are related to the same hazards or disasters such as earthquake, tsunami, fault, uplift, subsidence and mass-movement. In the last decade


H. El-Naggar et al. (Eds.): GeoMEast 2019, SUCI, pp. 88–106, 2020.
https://doi.org/10.1007/978-3-030-34252-4_8

major earthquakes occurred in several parts of the islands of Indonesia causing damages and many fatalities.

Indonesia has often been hit by huge disasters, such as earthquake and liquefaction. Earthquakes with magnitude ($M_w$) of 5.9 (2006), 7.6 (2009), 7 (2018) induced sand boiling and ground settlements in Yogyakarta, Padang, North of Lombok, respectively (Unjianto 2006; Tohari 2013; Kasbani 2018). Recently, the Palu earthquake occurred on 28 September 2018 with magnitude ($M_w$) of 7.4 caused strong shaking, generating a tsunami and massive liquefaction (GEER 2019). Therefore, increased attention should be focused on earthquakes and subsequent liquefaction potential in Indonesia.

In order to reduce the damage caused by an earthquake, the engineering profession needs to take into account the risks caused by seismic loading. Seismic loading is triggered by the earthquake vibration waves on the soil layer. Thus, it affects the soil behavior in order to support the structure, both structures beneath the soil or above.

Certain soils liquefy during earthquake shaking, losing its shear strength causing it to flow taking with it any overlying non-liquefied crust. As illustrated in Fig. 1. These soil layers drag the pile with them causing bending failure. In terms of soil-pile interaction, this mechanism assumes that the soil pushed the pile (Hamada and O'Rourke 1992; Finn and Fujita 2002). Soils that can liquefy are clearly understood and can be identified by evaluation procedures proposed by Youd et al. (2001). See "liquefaction assessment at foundation soil" further in this report.

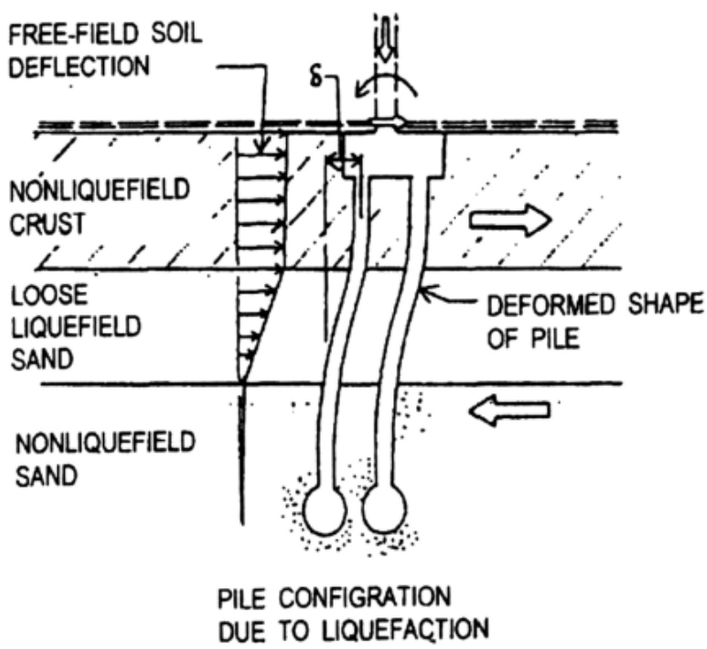


**Fig. 1.** Potential failure mode of piles due to seismic loading and soil liquefaction (Finn and Thavaraj 2001)

Foundations directly supported on soil are particularly vulnerable to liquefaction. This phenomenon is well understood and studied. Piled foundations and their response to liquefaction are less studied.

In structure terms, piles are slender columns with lateral support from the surrounding soil. Generally, as the length of the pile increases, the allowable load on the pile increases due to the additional shaft friction but the buckling load decreases inversely with the square of the length. If unsupported, these columns will fail due to buckling instability and not due to the crushing of the material. During earthquake-induced liquefaction, the soil surrounding the pile loses its effective confining stress and perhaps not offers sufficient lateral support. Hence, the pile now acts as an unsupported length column prone to axial instability. The instability may trigger the pile to buckle sideways in the direction of least elastic bending stiffness under the axial action load. In this case, the pile could push the soil and it could not be necessary to invoke lateral spreading of the soil to cause a pile to collapse (Bhattacharya 2003). If the pile buckles due to diminishing effective stress and shear strength owing to liquefaction, buckling instability can be a possible failure mechanism irrespective of the type of ground-level ground or sloping.

The mechanism and criteria to be used by practicing engineers are usually specified by prevailing codes. An example is bending failure assuming any non-liquefiable crust offers passive resistance and any liquefiable soil layer offers restraint equal to 30% of the overburden pressure (JRA 1996) as shown in Fig. 2. Furthermore, the Eurocode advises to design piles against bending due to inertia and kinematic forces arising from deformation of the surrounding soil (Bhattacharya 2003). It is required by the code to check separately against bending failure due to inertia load and not to add the effect of lateral spreading and inertia (Ishihara 1997). Unanimity among various researchers led to the assumption that lateral spreading is the cause of failure, such as Sato et al. (2001), Takahashi et al. (2002), Haigh (2002), Berrill (2001), Tokimatsu et al. (2001).

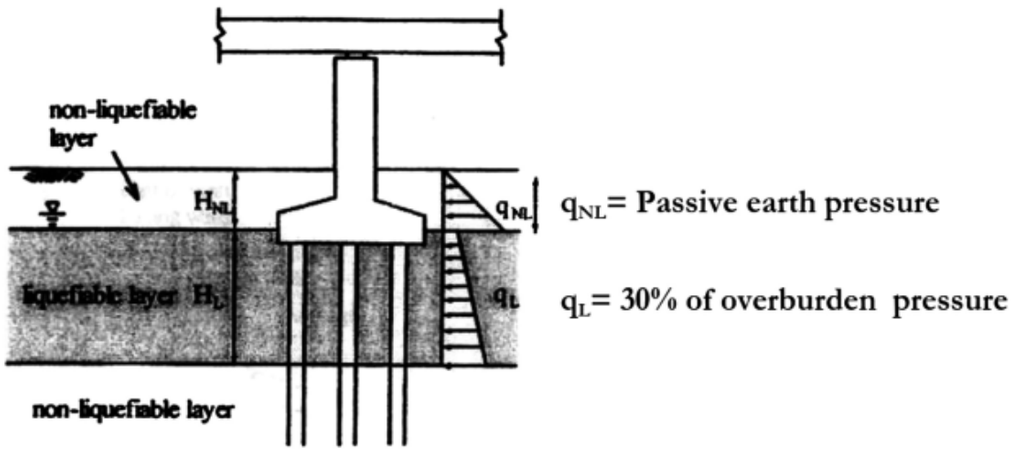


**Fig. 2.** The idealization for seismic design (JRA 1996)

## 2 Methodology

### 2.1 General Procedures for the Safety Assessment of Pile Foundations

Structures supported by piled foundations can be subjected to axial and lateral loadings. Structural failure of the pile can be seen in Fig. 3. Expected pile deformations under service loads and their ultimate load capacity are controlling factors in foundation design. There are several methods for calculating the bearing capacity of foundations including theoretical static analysis (Kulhawy 1984; Poulos 1989), procedures based on in situ test results (Meyerhof 1976; Fellenius 1997), dynamic methods (Rausche et al. 1985; Fellenius 2006), or interpretation of full scale pile load test (Fellenius 1990).

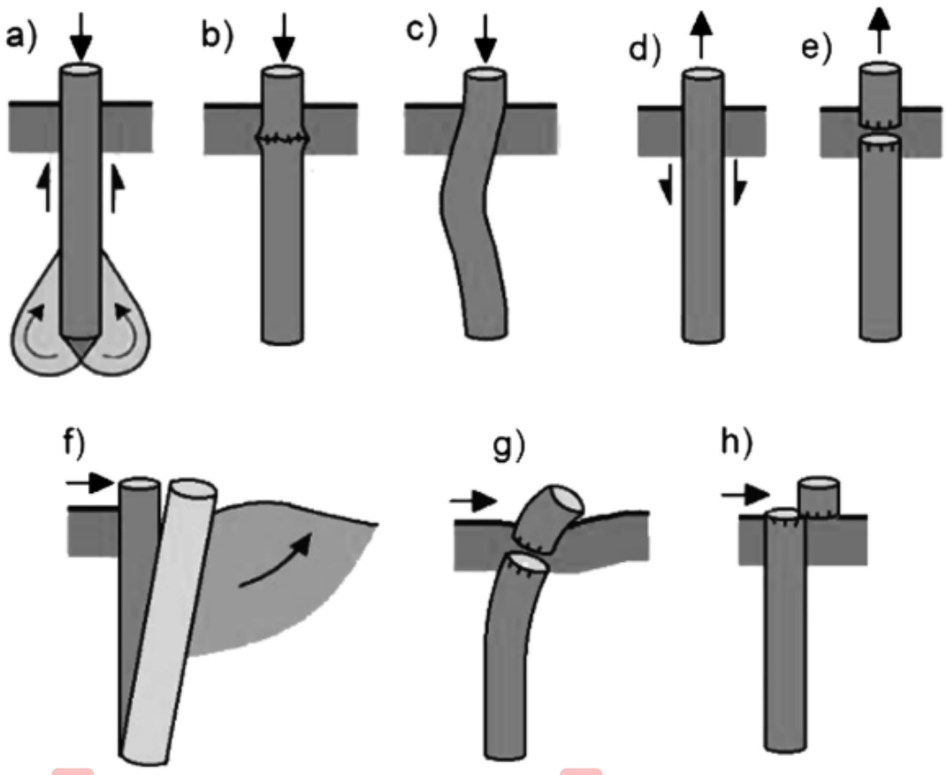


**Fig. 3.** Structural failure of the pile in different cases. (a)–(c) compression, (d), (e) tension, (f), (h) transverse (Wrana 2015)

### 2.1.1 Axial Bearing Capacity

The axial load capacity of the pile is derived from friction on the pile shaft and resistance at the pile tip. The ultimate bearing capacity $Q_u$ of a pile installed into sand can be expressed as Eq. (1):

$$Q_{uc} = Q_p + Q_s + W_{ds} - W_p \tag{1}$$

where point resistance is $Q_p$, shaft resistance is $Q_s$, weight of the pile is $W_p$, weight of the displaced soil is $W_{ds}$. For calculating pile capacity in tension, Eq. (2) is used:

$$Q_{ut} = Q_s + W_p \tag{2}$$

where $Q_{ut}$ is positive in tension and $Q_s$ is positive downwards. The end bearing $Q_p$ is taken zero in the case of tensile capacity. The pile weight, $W_p$ in both of the above equations, should be net pile weight, i.e., the total weight of the pile minus the total weight of the displaced soil and water.

### 2.1.2 Lateral Resistance

Several methods are available for determining the ultimate lateral resistance to pile in cohesionless soil (Hansen 1961; Broms 1964):

(1) Hansen (1961) presented an expression for predicting the ultimate lateral resistance to piles in a general $c - \phi$' soil, where $c$ and $\phi$' are the cohesion and the effective internal friction angle of the soil, respectively. For a cohesionless soil, $c = 0$ and the ultimate lateral resistance can be calculated by Eq. (3):

$$p_u = K_q \gamma z B \tag{3}$$

where $p_u$ is ultimate lateral resistance in the unit of force per pile length, $K_q$ is Hansen earth pressure coefficient which is a function of $\phi$', $\gamma$ is the effective unit weight of soil, $z$ is the depth from the ground surface and $B$ is diameter or width of the pile. The lateral deflections have been computed assuming that the coefficient of subgrade reaction increases linearly with depth.

(2) Broms (1964) suggested the ultimate lateral resistance in cohesionless soil as following Eq. (4):

$$p_u = 3K_q \gamma z B \tag{4}$$

where $K_p = 45^\circ + \phi'/2$ is passive earth pressure coefficient. Using Eq. (4), Broms (1964) prepared charts in a non-dimensional form giving the lateral capacity of piles in terms of the plastic moment and geometry of the pile.

## 2.2 General Procedure for the Safety Assessment of Piles in the Liquefied Ground

### 2.2.1 The Seismic Axial Capacity of Piled Foundations

The axial loading of piled foundations during earthquakes is complex, with the structure having to carry the vertical loads, which are applied under normal conditions, as well as additional axial load arising from the seismic excitation. A key feature of the end bearing capacity and shaft friction capacity was noted to be effective stress level in the soil profile, resulting in the loss of shaft friction and pile end bearing capacities as described by Knappett and Madabhushi (2008).

Bhattacharya (2006) indicated the static axial loading acting on each pile beneath the building is equally loaded during the static condition by neglecting any eccentricity of loading. During earthquake excitation, inertia action of the superstructure will impose dynamic loads on the piles, which can increase the total axial load on several piles, as given by Eq. (5):

$$P_{dynamic} = P_{static} + \Delta P = (1 + \alpha) P_{static} \tag{5}$$

Equation (5) needs the information of dynamic axial load factor $\alpha$, which is a function of the type, dimension and mass of the superstructure, the characteristics of seismic shaking, as well as material properties and geometry of the pile foundation.

### 2.2.2 Lateral Resistance in Liquefied Ground

The lateral resistance of liquefying sand in the field undoubtedly depends upon numerous factors that are not yet fully understood or readily quantifiable. These factors can reasonably be expected to include everything that affects the stress-strain response of saturated sand, including relative density, drainage conditions, relative magnitudes of monotonic and cyclic loading components, number of loading cycles, and soil characteristics (Wilson 2000).

Takahashi et al. (2002) conducted an experimental work to study the lateral resistance of pile in liquefied soil. The test results showed that the initial resistance to movement is negligible at all rates of loading but some resistance was mobilized after some amount of displacement.

### 2.2.3 Pile Buckling as Soil Liquefies

Structure design with column buckling and beam bending criteria require different approaches. The former is based on strength and the latter is on stiffness. Bending failure depends on the bending strength, for instance moment at first yield ($M_y$), and plastic moment capacity ($M_p$) of the pile. Whereas buckling represents a sudden instability of the pile when axial load reaches the critical value ($P_{cr}$) described by Dash et al. (2010).

Bhattacharya (2015) indicated the static axial load at which a frame supported on slender columns becomes laterally unstable is commonly known as the elastic critical load of the frame of buckling load. The elastic critical load of the pile is defined by Eq. (6):

$$P_{cr} = \frac{\pi^2 EI}{L_{eff}^2} \tag{6}$$

where $L_{eff}$ is the effective length of the column, which depends on the boundary condition at the column end i.e., fixed, pinned or free. The actual failure load $P_{failure}$ is therefore some factor $\phi$ ($\phi < 1$) times the theoretical Euler's buckling load given by Eq. (7):

$$P_{failure} = \phi P_{cr} \tag{7}$$

Based on Euler's theory, it may be inferred that buckling instability is initiated at around $\phi \doteqdot 0.35$.

As ground shaking starts, the excess pore pressure gradually increases which will in turn decrease the effective stress in the soil. As the effective stress of the soil approaches zero, the soil loses its strength and liquefies. Hence, the confining stress of the soil around the pile will be decreasing drastically, and eventually lead to buckling of the piles as shown in Fig. 4. Bending failure could be avoided by increasing the yield strength of the material. i.e. by using high-grade concrete or additional reinforcement, but it may not suffice to avoid buckling. To avoid buckling, there should be a minimum diameter depending on the depth of the liquefaction soil. In contrast, the pile has often being designed as a beam (Bhattacharya et al. 2004).

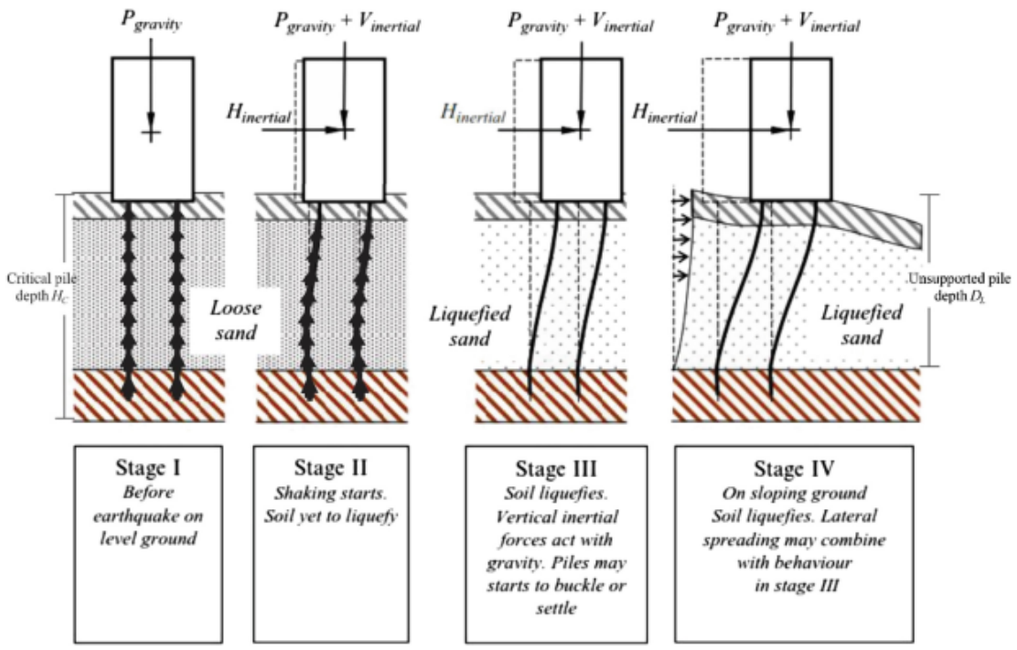


**Fig. 4.** Load applied to a pile foundation and failure mechanism (Bhattacharya 2015)

## 2.3 Analysis Procedures for Buckling Assessment of Piles Due to Soil Liquefaction

### 2.3.1 Liquefaction Assessment of Foundation Soil

Factors of safety against liquefaction could be computed using SPT-N based liquefaction evaluation procedure proposed by Youd et al. (2001). Liquefaction analysis calculates factors of safety against liquefaction at separated soil layer depths of a borehole. To address the severity of liquefaction for the entire borehole in the ground, the computed factors of safety and the associated depth intervals need to be considered. To evaluate the factor safety against liquefaction, both the soil's resistance to liquefaction and demand imposed on the soil by the earthquake need to be estimated. For the simplified approach used herein, the amplitude of cyclic loading is proportional to the peak ground acceleration (PGA) at the ground surface and the duration is related to the earthquake magnitude. The peak ground acceleration at SPT-N sites needs to be estimated for representative design earthquake.

The factor of safety against the initiation of liquefaction of a soil under a given seismic loading is generally defined as the ratio of cyclic resistance ratio (CRR), which is a measure of liquefaction resistance, over cyclic stress ratio (CSR), which is a representation of seismic loading that causes liquefaction. The term CSR is calculated in this paper as follows Eq. (8) (Youd et al. 2001):

$$CSR = 0.65\left(\frac{a_{max}}{g}\right)\left(\frac{\sigma_v}{\sigma_v'}\right)rd \tag{8}$$

where $\sigma_v$ is the vertical total stress of the soil at the depth considered, $\sigma_v'$ is the vertical effective stress, $a_{max}$ is the peak horizontal ground surface acceleration, $g$ is the acceleration of gravity, $r_d$ is the depth-dependent shear stress reduction factor (dimensionless). The term CRR is calculated using SPT-N data. The following empirical equation developed by Youd et al. (2001):

$$CRR = \left(\frac{1}{34 - N_{1,60,FC}} + \frac{N_{1,60,FC}}{135} + \frac{50}{(10N_{1,60,FC} + 45)^2} - \frac{1}{200}\right)MSF \tag{9}$$

where $N_{1,60,FC}$ is the SPT blow count normalized to an overburden pressure of 1 atm, a hammer efficiency of 60%, and correction of fines content. $MSF$ is the magnitude scaling factor for the adjustment of an earthquake magnitude of 7.5 to the magnitude of design earthquake of the site. The equation for factor of safety ($F_L$) against liquefaction is written as follows:

$$F_L = CRR/CSR \tag{10}$$

Iwasaki et al. (1982) developed the liquefaction potential index (LPI) to predict the potential of liquefaction to cause foundation damage at a site. The surface effect from liquefaction at depths greater than 20 m are rarely report, limited the computation of LPI to depth ($z$) ranging from 0 to 20 m. Proposed the following definition as Eq. (11):

$$LPI = \int_0^{20m} F.w(z)dz = \int_0^{20m} F.(10 - 0.5z)dz \tag{11}$$

In Eq. (11), $F = 1 - F_L$ for $F_L \leq 1$ and $F = 0$ for $F_L > 1$, where $F_L$ is obtained from simplified liquefaction evaluation procedure. $w(z)$ is depth-weighting. Thus, it is assumed the severity of liquefaction manifestation is proportional to (1) the thickness of liquefied layer; (2) the amount by which $F_L$ is less than 1.0; and (3) the proximity of the layer to the ground surface.

### 2.3.2 Unsupported Length Due to Liquefaction

The unsupported length of piles ($D_L$) indicated the extent along the pile where its lateral confining stress decrease significantly as a result of liquefaction of the surrounding soils. The unsupported length of piles is assessed based on the liquefaction profile. $D_L$ is equal to the thickness of liquefied soil layers plus additional distance necessary for fixity into the upper or lower non-liquefied soil layer. The fixity is typically three to five times the diameter of the pile (Bhattacharya and Goda 2013). In this case study, we adopt a fixity of five diameters of the pile.

### 2.3.3 Buckling Assessment of Piles

The buckling assessment of piles is obtained based on the critical pile length ($H_C$). We assume that each pile is equally loaded during static condition, the static load ($P_{static}$) acts on each pile under the building. During shaking, the inertia of the superstructure imposes the dynamic axial load on the piles. Thus, the piles with increased axial load are perhaps vulnerable to buckle.

The critical pile length describes the minimum length that the pile will buckle due to axial load based on Euler's theory. As indicated above, the critical pile length is evaluated by considering the static and dynamic axial load as well as the boundary conditions of the pile as given at Eq. (5).

To determine of critical pile length, the limit state condition of failure is assumed, $P_{dynamic} = P_{failure}$ and $L_{eff} = H_c$, and Eq. (7) can be rewritten as:

$$P_{dynamic} = \phi P_{cr} = \frac{\phi \pi^2 EI}{K^2 H_C^2} \tag{12}$$

where $EI$ is the bending stiffness of the pile and $K$ is the effective column length factor depending on the boundary condition of the pile. In this study, $\phi$ value of 0.35 and $K$ value of 1.0 are adopted in viewing that the pile head is fixed to the superstructure and the pile tip is embedded into the hard layer.

By rearranging Eq. (12), the critical pile length can be evaluated by Eq. (13):

$$H_C = \sqrt{\frac{0.35\pi^2 EI}{K^2 P_{dynamic}}} = \sqrt{\frac{0.35\pi^2 EI}{K^2(1+\alpha)P_{static}}} \tag{13}$$

Hence, liquefaction-induced pile buckling is indicated if $H_C < D_L$.

Finally, a buckling index $G$ is adopted as the difference between the critical pile length ($H_C$) for buckling and the unsupported length ($D_L$) due to liquefaction of foundation soils, where $H_C$ is the capacity variable and $D_L$ is the demand term. Thus, the failure criterion can be indicated by Eq. (14):

$$G = H_C - D_L \tag{14}$$

As shown in Fig. 5, if $G$ is greater than zero ($H_C > D_L$), then the pile is considered safe. Otherwise, the pile will be buckling due to seismic loading and soil liquefaction.

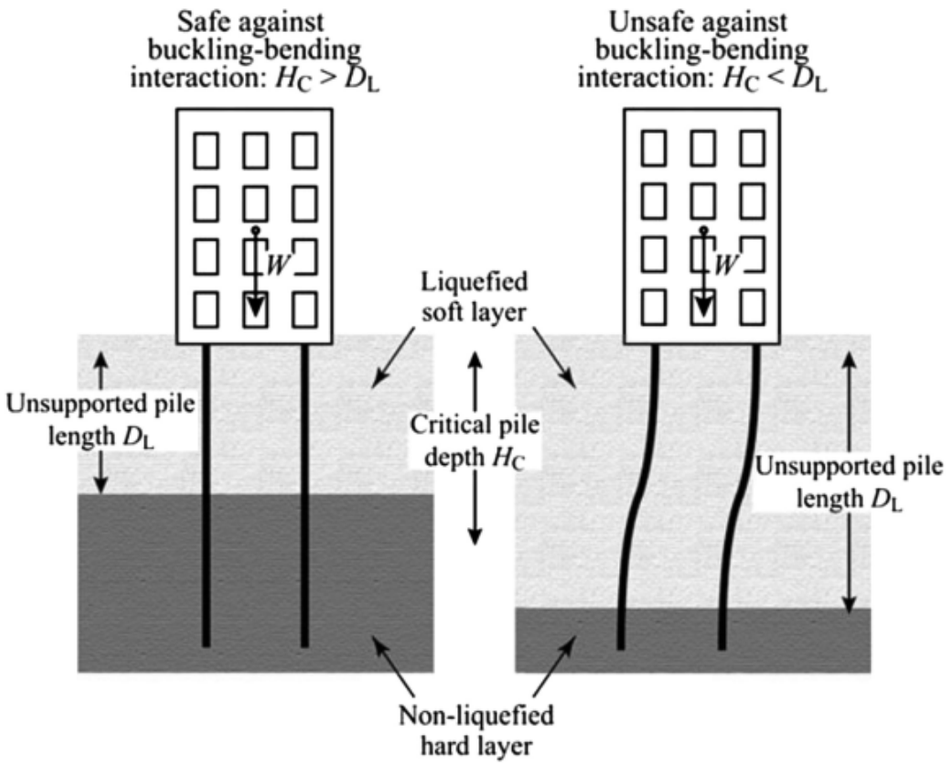


**Fig. 5.** Concept of critical length ($H_C$) and unsupported length ($D_L$), Bhattacharya (2015).

# 3 Case Study

## 3.1 Background Information

This case study related to a construction of a coal-fired power station in Central Java with capacity 2 × 1000 MW. In general, the project is located on an overlay alluvium deposit of the Muria mountain sediment material. The materials consist of coarse sand, fine sand, and clay. The soil contains old and recent river alluvial and shore deposits that were brought to the site by a small river flowing through and around the project site and tidal deposition. The upper soil deposits comprise alternating layers of very soft to soft clays and very loose to loose silty sands.

The case study covers 3 main facilities consisting of Boiler Units 5 & 6 and Central Control Building (CCB), which are supported by 1300, 1300, and 232 pre-stressed concrete piles, respectively. The piles are formed with exterior and interior diameters of 600 and 400 mm, respectively. The average pile length in Units 5 & 6 is 18 m, while in CCB is 12 m. The axial load for each pile ($P_{static}$) is 1450 kN, Young's modulus, $E$ is 33.9 GPa, flexural rigidity, $EI$ is 178 MN/m$^2$.

## 3.2 Liquefaction Analysis of the Ground

Several techniques on assessing liquefaction potential for the entire borehole depth have been proposed. The liquefaction potential of the site is evaluated based on the SPT-N approach by Youd et al. (2001) in association with the depth-weighted method by Iwasaki et al. (1982). As mentioned above, the earthquake with magnitude ($M_w$) of 6.8 and peak ground acceleration (PGA) of 0.210 $g$ are adopted in the analysis by Youd's method. The PGA is adopted from the Indonesian spectra design-Puskim, Ministry of Public Works (2011) database and consistent with the regional ground motion. Based on limited on-site data, an energy ratio of 70% is assumed for the current study, which is consistent with the value adopted by sub-contractor soil investigation for the SPT hammer used. In an analysis, the unit weight of soil at each of the material strata is based on the borehole data obtained at the time of drilling.

In the project site, there were several monitoring wells used to know the fluctuation of groundwater levels. This study assumes the groundwater levels recorded in the borehole logs and monitoring wells for the analysis during SPT test and liquefaction. In order to determine groundwater levels the average groundwater data for the area is separated into dry and wet seasons. To account for seasonal fluctuations, 1.40 m and 0.90 m below the ground surface are assumed as the average groundwater levels for dry and wet seasons, respectively. An increase in the groundwater level would decrease the effective stress of soil, which would, in turn enhance the computed seismic force (i.e., CSR) at the depth of interest. On the other hand, as a result of an increase in the groundwater level, a decrease in the effective stress of soil would amplify the over-burden pressure correction factor in order to accommodate the underestimated SPT-N due to rising groundwater, and thus cause an increase in the cyclic resistance ratio (CRR).

**Table 1.** *LPI* category and numbers of borehole

| LPI categories | Number of borehole computed | |
|---|---|---|
| | Wet season | Dry season |
| Low ($0 < LPI \leq 5$) | 6 | 7 |
| High ($5 < LPI \leq 15$) | 4 | 5 |
| Very high ($15 < LPI$) | 6 | 4 |
| Total | 16 | 16 |

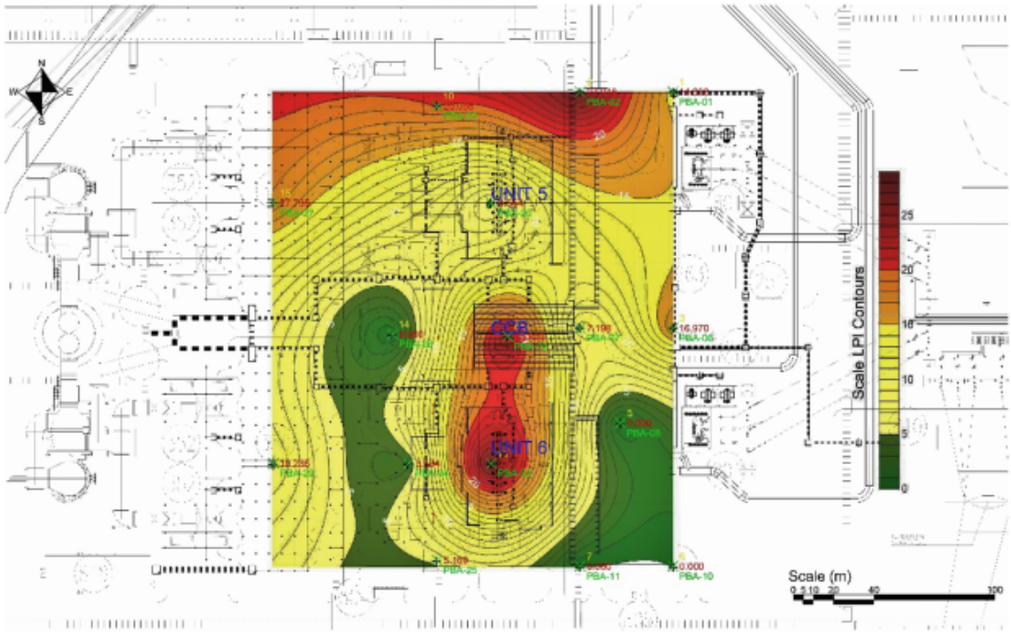


**Fig. 6.** *LPI* contours for groundwater scenario in wet season

Results of liquefaction potential and the unsupported pile length evaluation show the site is prone to liquefaction due to the design earthquake. Table 1 indicates the categories of liquefaction potential index (LPI) and the computed number of boreholes that cover the entire project site. Figure 6 shows LPI contour plots for the groundwater scenario during the wet season. The LPI results indicate more than 50% of the borehole with a LPI value greater than 5 (i.e., high to very high liquefaction potential) and the areas with high liquefaction potential generally fall in the center and southern parts of the site (CCB and Unit 6) and to north and east boundaries of Unit 5 (northern part of the site). The results of unsupported pile length from the representative 47 piles separated into 3 main facilities indicate more than 50% of the piles computed with $D_L$ value less than 5 m. The areas with $D_L$ value of more that 5 m generally fall in the center and southern part of the site, which are consistent with the LPI results with very high liquefaction potentials. These results are shown in Table 2 and Fig. 7.

**Table 2.** $D_L$ category and numbers of pile

| $D_L$ categories (m) | Number of pile computed | |
|---|---|---|
| | Wet season | Dry season |
| $D_L \leq 5$ | 29 | 26 |
| $5 < D_L \leq 10$ | 18 | 21 |
| $10 < D_L \leq 15$ | 0 | 0 |
| $15 < D_L$ | 0 | 0 |
| Total | 47 | 47 |

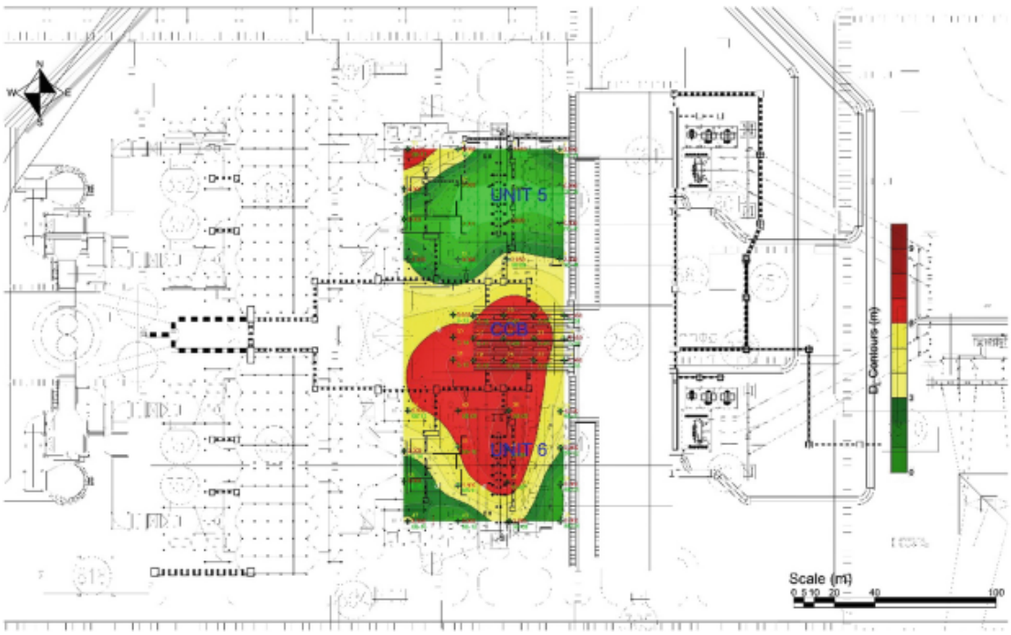


**Fig. 7.** $D_L$ contours for post-liquefaction in wet season.

### 3.3 Buckling Analysis of Piles

The pile buckling analysis can be divided into two phases, pre-liquefaction and post-liquefaction. Since the pile will normally not buckle due to the confinement of foundation soils prior to liquefaction, the post-liquefaction phase is therefore considered in the buckling assessment of the piles in this study.

In analyzing the dynamic axial load of pile ($P_{dynamic}$) as indicated in Eq. (5) and to estimate the additional dynamic axial load ($\Delta P$) on each of piles, the acting moment due to seismic shaking by the superstructure has to computed. Afterward, the moment can be distributed onto all of the resisting piles and the additional dynamic axial load on each of the piles can then be calculated.

Design provision BIS (2002) is the code of practice for estimating the force on the superstructure as well as the base shear, as given by:

$$V_B = C_s W \tag{15}$$

where $W$ is the total dead load from superstructure and $C_s$ is seismic response coefficient, for which $C_s$ could be computed by the four parameters (1) $Z$ is zone factor for maximum considered earthquake (MCE) (0.16; Prakash 2004; Bhatia et al. 1999), (2) $I$ is importance factor for the structure (1.5 for coal-fired power plants), (3) $R$ is response reduction factor, depending on the perceived seismic damage performance characterized by ductile or brittle deformations (4.0 for steel frame with concentric braces, (4) $Sa/g$ is the average response acceleration coefficient, which is a function on the site and vibration period on the structure. The spectrum acceleration can be estimated based on the fundamental period of the structure. For the post-liquefaction situation, the fundamental period the structure can be calculated by:

$$T_{post} = 2\pi\sqrt{\frac{W/g}{N_p \times 12EI/D_E^3}} \tag{16}$$

where $N_p$ is the total number of piles of the building, and is the depth to the lower boundary of liquefied soil plus and additional fixity. With the calculated fundamental period, the spectrum acceleration, and the base shear of the building as well, due to the design earthquake can then be obtained based on the design spectrum for the case of soft soil sites (BIS 2002).

In order to compute seismic moment on the superstructure, the arm where the inertial force acts can be estimated by the following:

$$ARM_{post} = D_E + \beta_3 H \tag{17}$$

where $H$ is the height of the building, and $\beta_3$ is the coefficient to account for the effective height where the inertia acts in a post liquefaction condition (typically, 0.5). Henceforth, the base shear and the arm, the acting moment can be computed as:

$$M_{post} = V_B ARM_{post} \tag{18}$$

The overall moment is then distributed to all of resisting piles of the superstructure for computing the additional dynamic axial load on each of the piles. To do this, the utmost dynamic load for piles located at the peripheral boundary of the pile foundation needs to be calculated first, and then the additional dynamic load of the inner piles can be estimated by assuming the dynamic load is proportional to the distance between the pile of concern and the axis of symmetry of the foundation area.

By the assuming a rectangular arrangement of piles ($n$ rows $\times$ $m$ columns) and the acting moment in the direction of row, the additional dynamic axial loads of the peripheral and inner piles can thus be computed, respectively, as follows:

$$\Delta P_{max} = \frac{x_{max} M_{post}}{2n\left(\sum_{i=1}^{max} x_i^2\right)} \tag{19}$$

$$\Delta P_i = \left(\frac{x_i}{x_{max}}\right) \Delta \mathrm{P}_{max} \tag{20}$$

where $x_{max}$ and $x_i$ are the distances of the peripheral and inner piles, respectively, to the axis of symmetry of the foundation area. Finally, the dynamic axial load ($P_{dynamic}$) can then be calculated by Eq. (5).

With the evaluated dynamic axial loads, Eq. (13) can be applied to estimate the critical length for each of the piles. Table 3 and Fig. 8 show the results of $H_C$ computations for the 47 representative piles that cover main facilities (Units 5 & 6 and CCB) of the site. The results indicate the minimum length that the on-site piles will buckle is 18 m, when the foundation soils are liquefied due to the design earthquake in wet season.

**Table 3.** $H_C$ category and numbers of pile

| $H_C$ categories (m) | Number of pile computed | |
|---|---|---|
| | Wet season | Dry season |
| $H_C \leq 5$ | 0 | 0 |
| $5 < H_C \leq 10$ | 0 | 0 |
| $10 < H_C \leq 15$ | 0 | 0 |
| $15 < H_C \leq 20$ | 34 | 34 |
| $20 < H_C$ | 13 | 13 |
| Total | 47 | 47 |

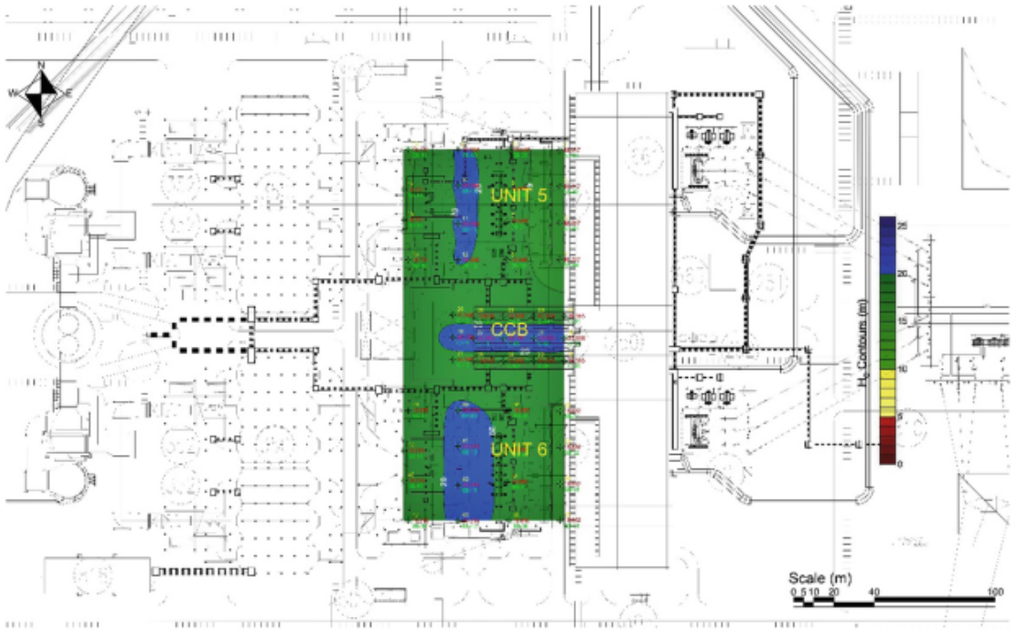


**Fig. 8.** $H_C$ contours for post-liquefaction in wet season

### 3.4 Buckling Index Computation

Based on the above the analyses on the unsupported pile length ($D_L$) due to liquefaction and the critical pile length ($H_C$), the buckling index ($G$) can hence be assessed to determine if the piles are adequate in resisting the buckling instability per Eq. (14). As stated previously, if a $G$ value is greater than zero then the pile is safe. Otherwise, the pile will be buckling. As shown in Table 4 and Fig. 9, the project site (Units 5 & 6 and CCB) will be safe from buckling instability, with calculated $G$ values of greater than 10 (m) and an average of $G$ value of 15 (m), for all of the piles at the project site.

**Table 4.** $G$ category and numbers of pile

| $G$ categories (m) | Number of pile computed | |
|---|---|---|
| | Wet season | Dry season |
| $G \leq -5$ | 0 | 0 |
| $-5 < G \leq 0$ | 0 | 0 |
| $0 < G \leq 5$ | 0 | 0 |
| $5 < G \leq 10$ | 0 | 0 |
| $10 < G$ | 47 | 47 |
| Total | 47 | 47 |

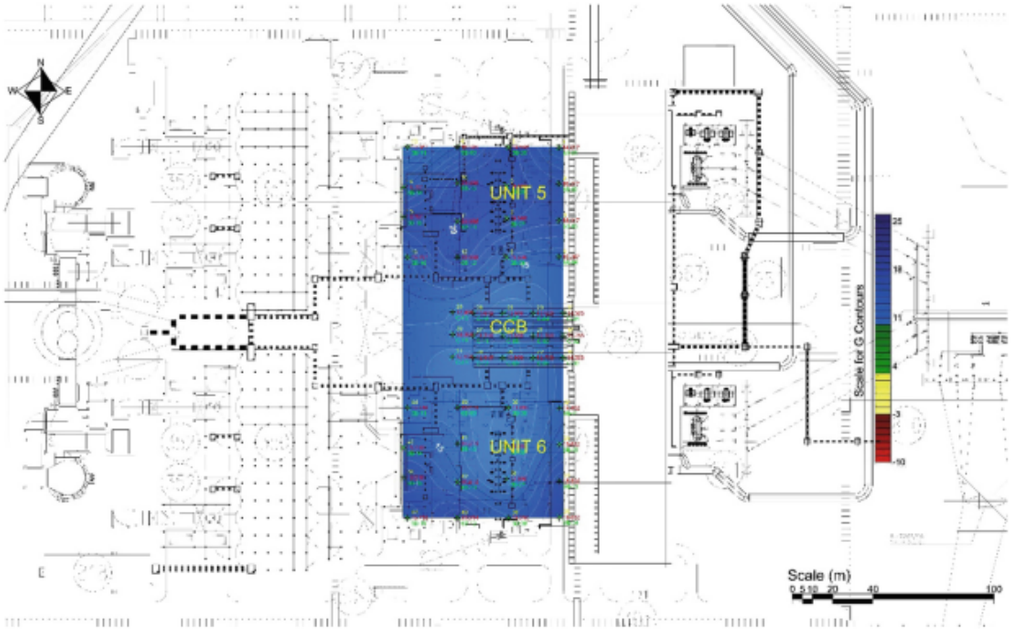


**Fig. 9.** *G* contours for post-liquefaction in wet season.

## 4 Conclusions

This study discusses the computation and assessment of liquefaction potential of foundation soils and buckling instability of piles for a coal-fired power station in Indonesia. Major findings of the study are listed as follows:

(1) Subsurface explorations reveal the soil deposit of the site generally consists of soft sandy silts or clays interbedded with loose fine sands to a depth of about 9 m. The deeper strata will be stiff and hard clayey soils.
(2) Liquefaction analysis indicates the foundation soils are prone to liquefaction due to design earthquake, with more than 50% of the boreholes assessed showing $LPI > 5$ (high to very high liquefaction potentials).
(3) Buckling assessment indicates the piles of the site will be safe from buckling failure, with computed critical pile lengths ($H_C$) of greater than 18 m and buckling indices ($G$) of greater than 10 (m), due to soil liquefaction by design earthquake, for the piles assessed at the project site.

**Acknowledgments.** The authors express their sincere thanks to Mr. Patrick W. Soule and Mr. Priya Purwanta for their contributions and review comments to this paper.

## REFERENCES


Berrill, J.B., Christensen, S.A., Keenan, R.P., Okada, W., Pettinga, J.R.: Case studies of lateral spreading forces on a piled foundation. Geotechnique **51**(6), 501–517 (2001)

Bhatia, S.C., Kumar, M.R., Gupta, H.K.: A probabilistic seismic hazard map of India and adjoining regions. Annali di Geofisica, No. **42**, 1153–1166 (1999)

Bhattacharya, S.: Pile Instability during Earthquake Liquefaction. Ph.D. thesis, University of Cambridge, UK (2003)

Bhattacharya, S.: Safety assessment of existing piled foundations in liquefiable soil against buckling instability. ISET. J. Earthq. Technol. **43**, 133–147 (2006)

Bhattacharya, S.: Safety assessment of piled buildings in liquefiable soils: mathematical tools. Encycl. Earthq. Eng. (2015). https://doi.org/10.1007/978-3-642-361975-5_232-1

Bhattacharya, S., Goda, K.: Probabilistic buckling analysis of axially loaded piles in liquefaction soil. Soil Dyn. Earthq. Eng. **45**, 13–24 (2013)

Bhattacharya, S., Madabhushi, S.P.G., Bolton, M.D.: An alternative mechanism of pile failure in liquefiable deposits during earthquakes. Geotechnique **54**, 203–213 (2004)

BIS. Indian Standard, Criteria for Earthquake Resistant Design of Structures, Part I. General Provisions and Buildings, Bureau of Indian Standards, New Delhi, India (2002)

Broms, B.B.: Lateral resistance of piles in cohesive soils. J. Soil Mech. Found. Div., ASCE **90** (2), 27–64 (1964)

Dash, S.R., Bhattacharya, S., Blakeborough, A.: Bending-buckling interaction as a failure mechanism of piles in liquefiable soils. Soil Dyn. Earthq. Eng. **30**, 32–39 (2010)

Fellenius, B.H.: Guidelines for Static Pile Design: A Continuing Education Short Course Text. Deep Foundations Institute, Hawthorne (1990)

Fellenius, B.H.: Piles subjected to negative friction: a procedure for design. Geotech. Eng. **28**(2), 277–281 (1997)

Fellenius, B.H.: The red book-basics of foundation design (2006). http://www.fellenius.net/

Finn, W.D.L., Thavaraj, T.: Deep foundations in liquefiable soils: case histories, centrifuge tests, and methods of analysis. In: Proceedings of the 4th International Conference on Recent Advances in Earthquake Geotechnical Engineering, San Diego, California, 26–31 March 2001

Finn, W.D.L., Fujita, N.: Piles in liquefiable soils: seismic analysis and design issues. Soil Dyn. Earthq. Eng. **22**(9), 731–742 (2002)

GEER (2019). Geotechnical reconnaissance: The 28 September 2018 M7.5 Palu-Donggala, Indonesia Earthquake. Geotechnical Extreme Events Reconnaissance

Haigh, S.K.: Effects of Earthquake-Induced Liquefaction on Pile Foundations in Sloping Ground, PhD thesis, University of Cambridge, UK (2002)

Hamada, M., O'Rourke, T.D.: Case studies of liquefaction and lifeline performance during past earthquakes. Volume 1, Japanese Case Studies, Technical Report NCEER92-0001, State University of New York at Buffalo, Buffalo, USA (1992)

Hansen, J.B.: The ultimate resistance of rigid piles against transversal forces. Bulletin No. 12, Danish Geotechnical Institute, Copenhagen, Denmark, pp. 5–9 (1961)

Ishihara, K.: Geotechnical aspects of the 1995 Kobe Earthquake. In: Proceedings of the 14th International Conference on Soil Mechanics and Foundation Engineering, Hamburg, Germany, pp. 2047–2073 (1997)

Iwasaki, T., Arakawa, T., Tokida, K.: Simplified procedures for assessing soil liquefaction during earthquakes. In: Proceedings of Soil Dynamics and Earthquake Engineering Conference, pp. 925–939 (1982)

JRA: Design Specifications of Highway Bridges, Part V: Seismic Design. Japan Road Association, Tokyo (1996)

Kasbani. The geological agency emergency response team found the North Lombok fault, Central Jakarta. Volcanology and Geological Disaster Mitigation, Geology Agency, Ministry of Energy and Mineral Resources of the Republic of Indonesia (2018). (in Indonesian)

Knappett, J.A., Madabhushi, S.P.G.: Liquefaction-induce settlement of pile groups in liquefiable and laterally spreading soils. J. Geotech. Geoenviron. Eng. **134**(11), 1609–1618 (2008)

Kulhawy, F.H.: Limiting tip and side resistance: fact or fallacy. In: Meyer, R.J. (ed.) Proceedings of Symposium on Analysis and Design of Pile Foundations, San Francisco, American Society of Civil Engineers, New York, pp. 80–89 (1984)

Meyerhof, G.G.: Bearing capacity and settlement of pile foundations. J. Geotech. Eng. Div. ASCE **102**(3), 195–228 (1976)

Ministry of Public Works. Indonesian Design Spectra Application, Center Settlement Research & Development, Indonesia (2011). (in Indonesian)

Poulos, H.G.: Pile behavior-theory and application. Geotechnique **39**(3), 365–415 (1989). https://doi.org/10.1680/geot.1989.39.3.365

Prakash, V.: Whither performance-based engineering in India, ISET. J. Earthq. Technol. **41**(1), 201–222 (2004)

Rausche, F., Goble, G.G., Likins, G.: Dynamic determination of pile capacity. J. Geotech. Eng. **111**(3), 367–383 (1985)

Sato, M., Ogasawara, M., Tazoh, T.: Reproduction of lateral ground displacements and lateral-flow earth pressures acting on a pile foundations using centrifuge modelling. In: Proceedings of the 4th International Conference on Recent Advances in Geotechnical Earthquake Engineering and Soil Dynamics and Symposium in Honour of Professor W.D. Liam Finn, San Diego, California, 26–31 March 2001 (2001)

Takahashi, A., Kuwano, Y., Yano, A.: Lateral resistance of buried cylinder in liquefied sand. In: Proceedings of the International Conference on Physical Modelling in Geotechnics, ICPMG-02, St. John's, Newfoundland, Canada, 10–12 July (2002)

Tohari, A.: Characteristic of passive liquefaction in the Padang City based on the microtremor method. In: Proceedings of the Results Presentation of the Research at the Geological Research Center, Indonesian Institute of Sciences, LIPI. Bandung (2013). (in Indonesian)

Tokimatsu, K., Suzuki, H., Suzuki, Y.: Back-calculated p-y relation of liquefied soils from large shaking table tests. In: Proceedings of the 4th International Conference on Recent Advances in Geotechnical Earthquake Engineering and Soil Dynamics and Symposium in Honour of Professor W.D. Liam Finn, San Diego, California, 26–31 March 2001 (2001)

Unjianto, B.: The worst damage from the earthquake on Merapi Mountain sediment deposit. Suara Merdeka Cyber News (2006). (in Indonesian)

Wilson, D.W., Boulanger, R.W., Kutter, B.L.: Observed seismic lateral resistance of liquefiying sand. J. Geotech. Geoenviron. Eng. **126**(10), 898–906 (2000)

Wrana, B.: Pile load capacity-calculation methods. Studia Geotechnica et Mechanica, vol. 37, no. 4 (2015). https://doi.org/10.1515/sgem-2015-0048

Youd, T.L., et al.: Liquefaction resistance of soil: summary report from 1996 NCEER & 1998 NCEER/NSF workshops on evaluation of liquefaction resistance of soils. J. Geotech. Geoenviron. Eng., ASCE **127**(10), 817–833 (2001)

# A Case Study on Buckling Stability of Piles in Liquefiable Ground for a Coal-Fired Power Station in Indonesia

ORIGINALITY REPORT

| 11% | 6% | 9% | 5% |
|---|---|---|---|
| SIMILARITY INDEX | INTERNET SOURCES | PUBLICATIONS | STUDENT PAPERS |

PRIMARY SOURCES

| | | |
|---|---|---|
| 1 | Malhotra, Sanjeev. "Axial Load Capacity of Pipe Piles in Sand: Revisited", Deep Foundations 2002, 2002.<br>Publication | 1% |
| 2 | mts.intechopen.com<br>Internet Source | 1% |
| 3 | Submitted to University of Leeds<br>Student Paper | 1% |
| 4 | Yu Huang, Miao Yu. "Hazard Analysis of Seismic Soil Liquefaction", Springer Science and Business Media LLC, 2017<br>Publication | 1% |
| 5 | coek.info<br>Internet Source | 1% |
| 6 | www.eng.ox.ac.uk<br>Internet Source | 1% |
| 7 | Submitted to Fiji National University<br>Student Paper | <1% |
| 8 | Submitted to Liverpool John Moores University<br>Student Paper | <1% |
| 9 | Md. Shakhawat Hossain, A. S. M. Maksud Kamal, Md. Zillur Rahman, Atikul Haque Farazi et al. "Assessment of soil liquefaction potential: a case study for Moulvibazar town, Sylhet, Bangladesh", SN Applied Sciences, 2020 | <1% |

Publication

| | | |
|---|---|---|
| 10 | Springer Series in Geomechanics and Geoengineering, 2008.<br>Publication | <1 % |
| 11 | www.scribd.com<br>Internet Source | <1 % |
| 12 | "Geotechnics and Earthquake Geotechnics Towards Global Sustainability", Springer Science and Business Media LLC, 2011<br>Publication | <1 % |
| 13 | Bogumił Wrana. "Pile Load Capacity – Calculation Methods", Studia Geotechnica et Mechanica, 2015<br>Publication | <1 % |
| 14 | Submitted to Universitas Negeri Semarang<br>Student Paper | <1 % |
| 15 | www.mdpi.com<br>Internet Source | <1 % |
| 16 | www.researchgate.net<br>Internet Source | <1 % |
| 17 | Submitted to University of Surrey<br>Student Paper | <1 % |
| 18 | Koichi Hayashi. "Seismic investigations in residential area liquefied by Mid Niigata Prefecture Earthquake", SEG Technical Program Expanded Abstracts, 2006<br>Publication | <1 % |
| 19 | Submitted to University of Stellenbosch, South Africa<br>Student Paper | <1 % |
| 20 | ebin.pub<br>Internet Source | <1 % |
| 21 | George Papathanassiou, Kostas Seggis, Spyros Pavlides. "Evaluating earthquake- | <1 % |

induced liquefaction in the urban area of Larissa, Greece", Bulletin of Engineering Geology and the Environment, 2010
Publication

---

22 Kashif Quamar Inqualabi, Rajeev Kumar Garg, K. Balaji Rao. "Seismic Vulnerability of Urban Bridges Due to Liquefaction Using Nonlinear Pushover Analysis and Assessing Parameters for Damage Detection", Procedia Engineering, 2017 <1%
Publication

---

23 Zhang, L.. "Nonlinear analysis of laterally loaded rigid piles in cohesionless soil", Computers and Geotechnics, 200906 <1%
Publication

---

| | | | |
|---|---|---|---|
| Exclude quotes | On | Exclude matches | < 10 words |
| Exclude bibliography | On | | |

# A Case Study on Buckling Stability of Piles in Liquefiable Ground for a Coal-Fired Power Station in Indonesia

GRADEMARK REPORT

FINAL GRADE

/0

GENERAL COMMENTS

**Instructor**

PAGE 1

PAGE 2

PAGE 3

PAGE 4

PAGE 5

PAGE 6

PAGE 7

PAGE 8

PAGE 9

PAGE 10

PAGE 11

PAGE 12

PAGE 13

PAGE 14

PAGE 15

PAGE 16

PAGE 17

PAGE 18

PAGE 19